Korean J. Chem. Eng., **28**(1), 232-238 (2011)
DOI: 10.1007/s11814-010-0444-8

Oriented crystallization of xanthine derivatives sublimated on self-assembled monolayers

Jihae Chung and Il Won Kim†

Department of Chemical and Environmental Engineering, Soongsil University, Seoul 156-743, Korea
(*Received 18 September 2010 • accepted 5 October 2010*)

Abstract−The oriented crystallization of caffeine and theobromine on self-assembled monolayers (SAMs) is reported. The SAMs were prepared by reacting 1-decanethiol, 11-mercapto-1-undecanol, or 11-mercaptoundecanoic acid on flat Au surfaces to form methyl, hydroxyl, or carboxylic acid functionalities on the substrates. Crystallization was conducted by sublimating the xanthine alkaloids on the SAMs. X-ray diffraction and morphology observation/simulation were combined to identify the preferred orientation of caffeine and theobromine crystals. Also, the identified crystal orientation was examined through molecular models to understand the nature of the interfacial interactions that direct the nucleation process. CH/π interaction as well as strong hydrogen bonding appeared to act as the specific interactions to control the molecular orientation of caffeine and theobromine in stereochemically determined manners that persisted during the crystallization process. More importantly, the stability of the orientational regulation showed a clear correlation to the cohesiveness of the xanthine molecular layer parallel to the nucleating substrate. We believe this indicates that the structural coherence of the precursors or nuclei of the crystallization is essential to effectively utilize the interfacial interactions in a cooperative manner to firmly control the crystal orientation.

Key words: Crystallization, Nucleation, Xanthine, Sublimation, Self-assembled Monolayer

INTRODUCTION

Biominerals have induced many interests in crystallization communities because of their unusually well controlled processes of crystal formation [1]. In biological crystallization, organic biomacromolecules associated with inorganic biominerals are the key controlling agents responsible for the elegant regulation of crystal nucleation and growth [2]. The biomacromolecules seem to possess abilities to stimulate, restrict, and guide the assembly of the constituents of biominerals, which ultimately translate into the exquisite control of the size, shape, orientation, and polymorphs of biominerals.

Notable examples include the nacreous shell of the red abalone (*Haliotis rufescens*), the dorsal arm plate of the brittle star (*Ophiocoma wendtii*), and the coccolith scale of the coccolithophore (*Emiliania Huxleyi*). Abalone nacre consists of stacked micro-plates, which are in turn made by nano-grains of metastable aragonite crystals [3,4]. Brittle star plate has elaborately structured micro-lenses, while the entire framework still forms as a calcite single crystal [5]. Coccolith plate is intricately assembled by multiple calcite single crystals, each of which has hammer-headed shape formed by directional crystal growth [6].

These observations of exquisitely structured biominerals have provided opportunities to generate new paradigms, or reexamine traditional notions, of crystallization. Especially fruitful investigations have been made in terms of interfacial relationships between the minerals and biomolecules. First, biomolecules, acting as additives to regulate crystallization kinetics, are associated with acceleration and inhibition of molecular step growth [7-9]. In addition, they appear to be involved with stabilization of specific polymorph or phase of biominerals, presumably being operative on phase transformation control delineated by Ostwald rule of stages [10,11]. Second, biomacromolecules, working as substrates to guide crystal nucleation, are correlated with the oriented crystal growth [2,12]. Moreover, structured biomacromolecules appear to manage bio-crystallizer space to assist an additional level of crystallization control [1, 2,6]. Finally, biomolecules, influencing biomineral growth in a stereochemically specific manner, are related not only to the nucleation of specific crystal planes but also to the growth modification manifested in shape changes [13,14]. These studies have also been expanded into bio-inspired and biomimetic crystallization, where oriented crystal growth, depending on the molecular structures of nucleating surfaces, is further engineered by supplementary additives [15,16].

The orientation-controlled crystal growth mediated by the stereochemical interaction is especially interesting because one-dimensional orientation of crystals with respect to the nucleating substrates is often found when an epitaxial match does not exist between the crystals and substrates [15]. Most likely explanation for this phenomenon appears to be the directional interactions in the molecular level between the substrates and crystals, while ledge-induced crystallization or graphoepitaxy can be postulated as an alternative explanation [15-18]. In this regard, studies involving self-assembled monolayers (SAMs) are most revealing. Electrostatic interactions have proven effective for nucleation of specific planes of inorganic and organic crystals [15,19]. Strong hydrogen bonding is also shown to be an influential interaction to induce oriented nucleation of organic crystals [20]. While these strong specific interactions are conceivably the most reliable interfacial interactions for the nucleation of specified crystal planes, the role of less strong interaction is not well understood.

†To whom correspondence should be addressed.
E-mail: iwkim@ssu.ac.kr

Non-conventional hydrogen bonding is one of the interactions that are weaker than the previously mentioned examples, nevertheless playing important roles in subtle fine-tuning of crystallization. This interaction involves weak donors and/or weak acceptors of hydrogen bonding. Some examples for weak donors are -SH, -PH, and -CH, and those for weak acceptors are -CF, C=C, and π [21]. The instances where weak hydrogen bonds are important are increasingly recognized in crystals of proteins. For example, the hydrogen bonds with π-acceptors are well documented in protein crystals especially when the side chain of tryptophan is involved [22]. Equally abundant examples are present for weak hydrogen bonds in small organic molecules [21]. For instance, additional CH$\cdots\pi$ interactions for the $\pi\cdots\pi$ stacking 2,2′:6′,2″-terpyridine molecules prompt the formation of monoclinic polymorph, whereas their absence leads the crystallization of orthorhombic polymorph [23,24].

In the present study, SAM with functional end groups of -CH_3 (SAM-CH_3 from 1-decanethiol on Au) was compared with those with -COOH (SAM-COOH from 11-mercaptoundecanoic acid on Au) and -OH (SAM-OH from 11-mercapto-1-undecanol on Au) to reveal the role of the weak interactions in the oriented nucleation of organic crystals. Caffeine and theobromine were chosen as the growing crystals because of their possibility of weak interactions as well as strong hydrogen bonding with the end groups of SAMs. Also, caffeine and theobromine have nearly the same molecular structures to enable systematic investigation by comparing their crystallization on SAMs. They are both xanthine alkaloids with the difference of one additional methyl group to the caffeine molecule. Their crystal structures are quite different because of this subtle difference. Crystalline theobromine ($P2_1/c$, monoclinic, a=9.2890 Å, b=18.698 Å, c=9.0381 Å, β=91.75°) exists in a dimer structure that possesses strong hydrogen bonding between two theobromine molecules via double NH$\cdots$O=C interactions. [25] In contrast, α polymorph of caffeine (R-3c, hexagonal, a=b=14.830 Å, c=6.7648 Å) has a rotational disorder, lacking similar hydrogen bonding between molecules [26]. Still, they possess carbonyl groups and π-conjugated purine rings in common, which can interact with the end groups of SAMs in a similar fashion.

EXPERIMENTAL

SAMs, where crystal growth was induced afterward, were prepared as follows. Au (ca. 6 μm) was sputter-coated (Cressington Sputter Coater 108) on a small piece of Si wafer (Buycemi; Suwon, Korea), which had been thoroughly cleaned by successively washing with acetone, absolute ethanol, and deionized water. Then, it was glued on a clean glass slide using a UV-curable adhesive (Norland optical adhesive 81; Norland products, Inc., Cranbury, NJ). Ultra flat Au surface in contact with Si wafer was exposed by delaminating the Si layer. The prepared Au surface exhibited high flatness with RMS roughness <0.2 nm measured by atomic force microscopy (MFP3D-SA, Asylum research; Santa Barbara, CA). (Note that the RMS roughness of the Si wafer was <0.1 nm measured by the same method.) It was immediately placed into a thiol solution (1.0 mM) prepared in absolute ethanol (99.9%, Samchun Chemical; Seoul, Korea). 1-Decanethiol (96%, Aldrich) 11-mercapto-1-undecanol (97%, Aldrich), and 11-mercaptoundecanoic acid (95%, Aldrich) were used to prepare each thiol solution to form SAMs with -CH_3, -OH, and -COOH functional groups. The successful SAM formation was tested by measuring contact angle with deionized water (DSA 100, Krüss; Hamburg, Germany). SAMs with -CH_3, -OH, and -COOH showed contact angles of ca. 101, 17, 53°, respectively. Caffeine (>98.5%, Aldrich) and theobromine (>99.0%, Sigma) crystals were formed on the SAM substrates by sublimating from heated surfaces (150 °C and 240 °C, respectively).

Sublimation sources were prepared by spreading ca. 2 mg fine powders on ca. 0.5 cm×0.5 cm area of the heated surfaces. The SAM substrates were positioned 1 cm above the sublimation sources, and the other sides, glass, were exposed to room temperature atmosphere to induce natural cooling of the substrates. Crystal growth was for 15 min, after which the substrate was immediately removed from the crystal growth system. Crystals grown on the SAMs were characterized by scanning electron microscopy (SEM: JSM-6250A, Jeol) and X-ray diffraction (XRD: AXS D5005 X-ray diffractometer, Bruker). SEM was performed after thin Au coating to minimize surface charging. XRD was performed in the θ-2θ mode (5-40°, 2°/min; Cu Kα radiation generated at 40 kV and 40 mA) to study orientation of the crystals as well as their crystallographic identity. Mercury (version 2.3; The Cambridge Crystallographic Data Centre, Cambridge, UK), CrystalMaker (version 6.3.5; CrystalMaker Software Ltd, Oxfordshire, UK), and Shape (version 6.0; Shape Software, Kingsport, TN, USA) software was used along with the known crystallographic information to investigate molecular models, X-ray reference peaks, and crystal morphologies.

RESULTS AND DISCUSSION

Caffeine formed as needle-shaped crystals on SAMs, and their length and thickness were mostly in the range 10-20 micron and 2-3 micron, respectively (Fig. 1). While the overall shape of the crystals was similar on all three SAMs, their orientation was clearly different. On SAM-CH_3, ca. 60% caffeine needles formed with their cross-sectional surface in contact with the nucleating substrates, thus revealing their hexagonal cross-sections on the other end of the crystals, although their angular orientation with respect to the substrate appeared to vary to a certain degree (Fig. 1(a)). Also, we noted that terminal morphology was not very well defined possibly because of the disordered structure in caffeine crystals [26]. The other fraction of the needles had their long axis parallel to the nucleating substrates. On SAM-COOH and SAM-OH, nearly all caffeine needles were formed with their long-axis side surfaces in contact with the nucleating substrates (Figs. 1(b) and 1(c)). Crystals on SAM-COOH and SAM-OH appeared to have similar orientation with respect to each substrate, and many of these crystals did not possess clear-cut end morphology as observed for those on SAM-CH_3.

Theobromine crystals formed as truncated pyramids on SAM-CH_3 (Fig. 1(d)), but those on SAM-COOH and SAM-OH are not as well expressed (Figs. 1(e) and 1(f)). On SAM-CH_3, truncated pyramids displayed their cut surfaces nearly parallel to the nucleating substrate (Fig. 1(d)). On SAM-COOH and SAM-OH, the orientation of the crystals appeared relatively irregular. Fig. 1(e) shows crystals on SAM-COOH, where ca. 20% crystals appear similar to those on SAM-CH_3, and other fraction of crystals are more tilted or completely dissimilar in their orientation and morphology. Fig.

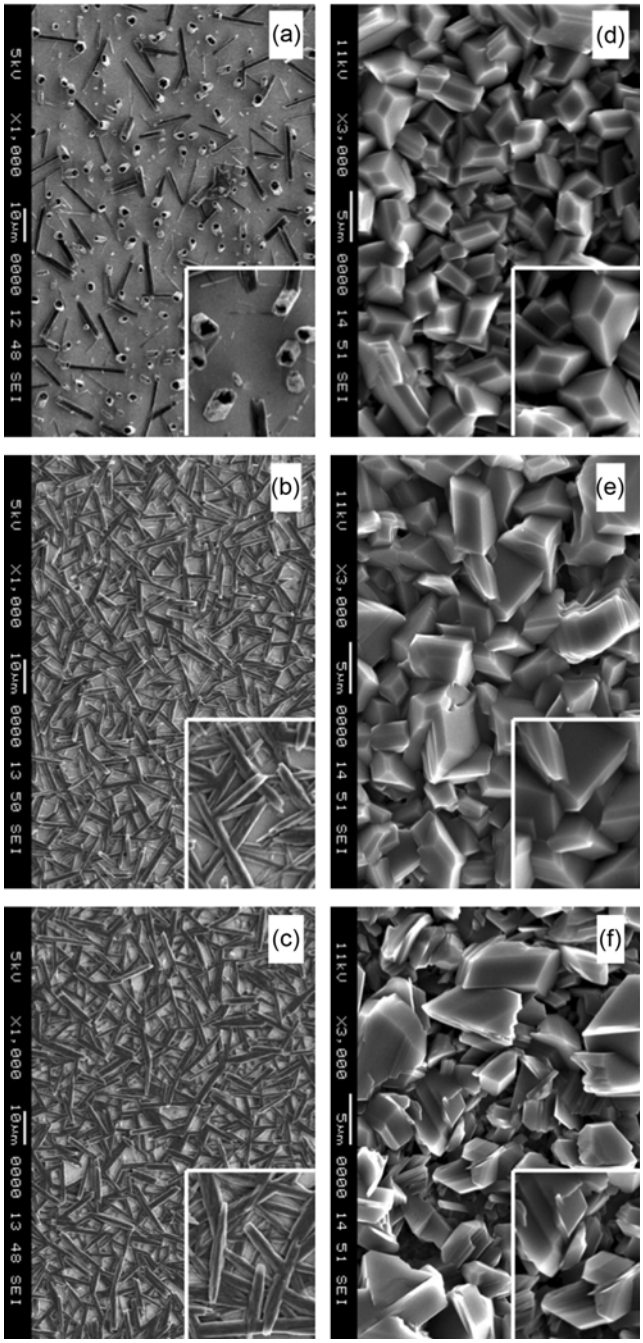

Fig. 1. Caffeine and theobromine crystals grown on SAMs. (a) Caffeine on SAM-CH_3, (b) caffeine on SAM-COOH, (c) caffeine on SAM-OH, (d) theobromine on SAM-CH_3, (e) theobromine on SAM-COOH, and (f) theobromine on SAM-OH.

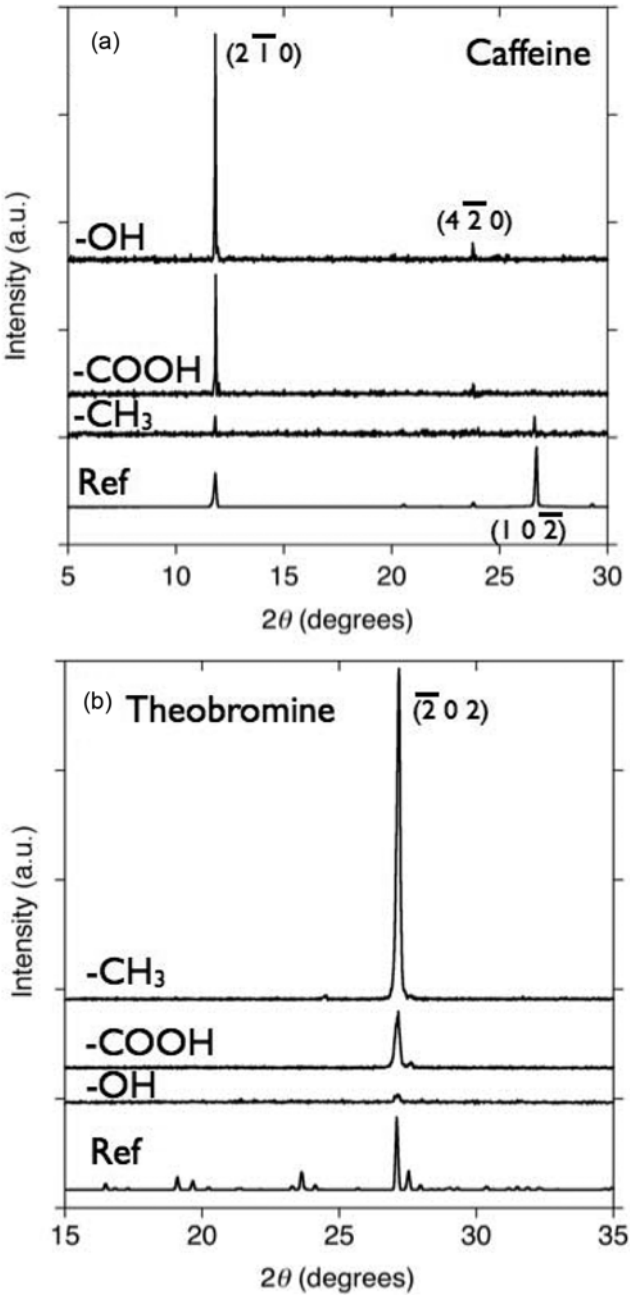

Fig. 2. X-ray diffraction patterns observed for (a) caffeine and (b) theobromine crystals on SAMs in the θ-2θ mode to qualitatively distinguish the preferred orientations. Reference pattern is also shown at the bottom for comparison.

1(f) shows crystals on SAM-OH, where crystals bear almost no resemblance in their orientation and morphology to those on SAM-CH_3. We also noted that repeated experiments confirmed the robust orientational growth for theobromine crystals on SAM-CH_3, but not for those on SAM-COOH and SAM-OH, where the degree of the orientational divergence (or randomness) was also difficult to assess.

XRD also confirmed the SEM observation of caffeine and theobromine crystals on SAMs (Fig. 2). XRD was performed in the θ-2θ mode to qualitatively reveal the preferred orientation of the crystals with respect to the nucleating SAMs [15,27]. Caffeine crystals (Fig. 2(a)) on SAM-OH showed a distinctively prominent (2 −1 0) peak. Those on SAM-COOH exhibited similar diffraction patterns. In contrast, caffeine needles on SAM-CH_3 revealed newly appeared (1 0 −2) diffraction peak, while the intensity of the (2 −1 0) peak was significantly reduced. This qualitatively corroborated the SEM observation, where caffeine needles were lying down on SAM-OH and SAM-COOH in a similar fashion, and more than

half of the crystals were standing on SAM-CH_3 revealing their hexagonal cross-sections (The molecular orientation is analyzed in detail later in this paper.).

Theobromine crystals on SAMs had (−2 0 2) as the most distinctive diffraction plane (Fig. 2(b)). Among the SAM substrates in the present study, SAM-CH_3 induced crystal growth that displayed the strongest (−2 0 2) peak. SAM-COOH and SAM-OH produced crystals that showed much reduced intensity of the (−2 0 2) peak. In three independently repeated experiments, the (−2 0 2) diffraction intensity was always strongest for the theobromine crystals on SAM-CH_3. The repeated experiments also confirmed the (−2 0 2) intensity reduction for those on SAM-COOH and SAM-OH, while the relative extent of intensity reduction was not well preserved. Again, this result qualitatively corroborated the SEM observation, where nearly all theobromine crystals standing on SAM-CH_3 were truncated pyramidal to display cut surfaces nearly parallel to the substrate, and those on SAM-COOH and SAM-OH showed much less defined morphology and orientation. For the particular set of samples shown in Figs. 1(e) and 1(f), only less than a quarter of crystals on SAM-COOH were in similar morphology and orientation to those on SAM-CH_3, while equivalent crystals were hard to find on SAM-OH. This observation is in good correlation to the (–2 0 2) diffraction intensity shown in Fig. 2(b) (Detailed analysis of the molecular orientation is given in the later part of this paper.).

Crystal morphology was simulated to reconcile the SEM and XRD observations (Fig. 3), using the crystallographic information known for the α polymorph of caffeine and the crystalline theobromine. Crystals on SAM-CH_3 were chosen because they were better defined to give out more information about their morphology. Fig. 3(a) shows the SEM micrograph (same as the inset of Fig. 1(a)) and the simulated morphology of three selective caffeine crystals. The standing needle-shaped crystals wrapped by six equivalent {2 −1 0} side faces are consistent with the decreased intensity of the (2 −1 0) X-ray diffraction as well as the morphological observation. Note that the end morphology of experimentally obtained caffeine needles was not very well defined, possibly because of the disordered structure in caffeine crystals [26]. Fig. 3(b) shows the SEM micrograph (same as the inset of Fig. 1(d)) and the simulated mor-

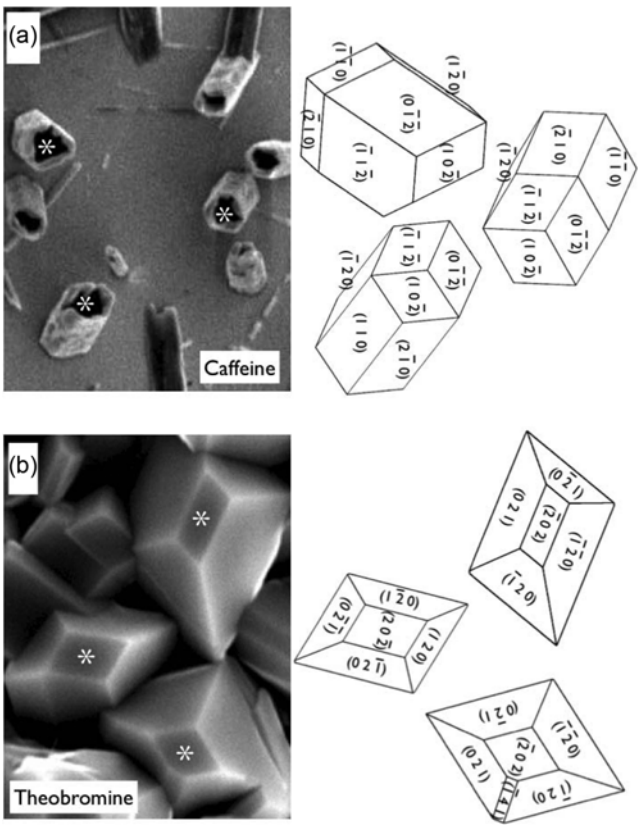

Fig. 3. SEM micrographs (left) and schematic representations (right) of the (a) caffeine and (b) theobromine crystals grown on SAM-CH_3.

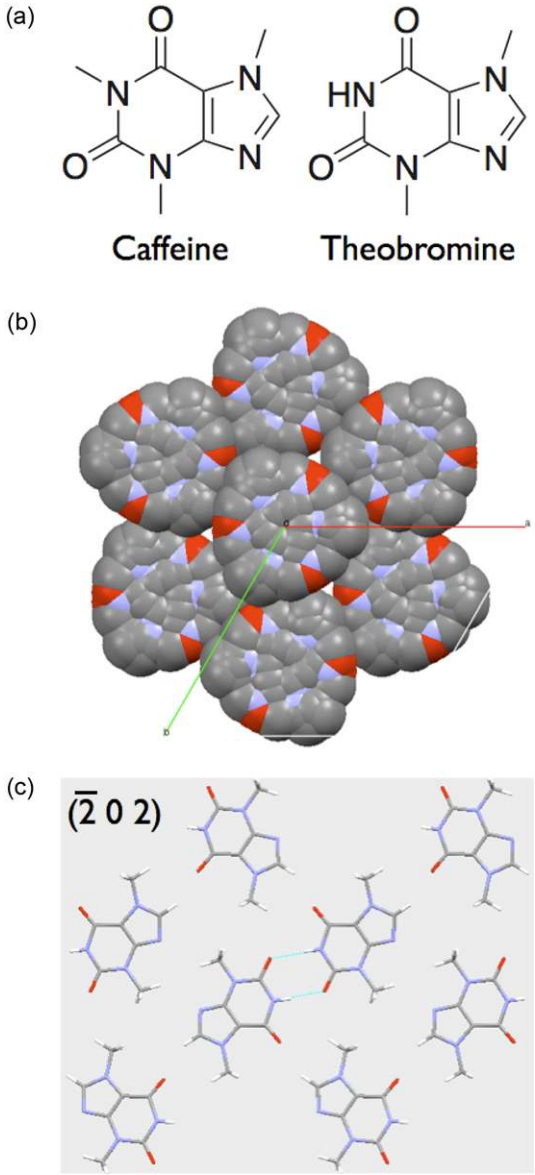

Fig. 4. Structures of caffeine and theobromine: (a) chemical structures, (b) disordered caffeine (α polymorph) molecules π-stacked along the c-direction (redrawn following reference 26), (c) two-dimensional network in crystalline theobromine nearly parallel to (–2 0 2) plane (grey square) [25]. Dimer forming hydrogen bonds are indicated in turquoise.

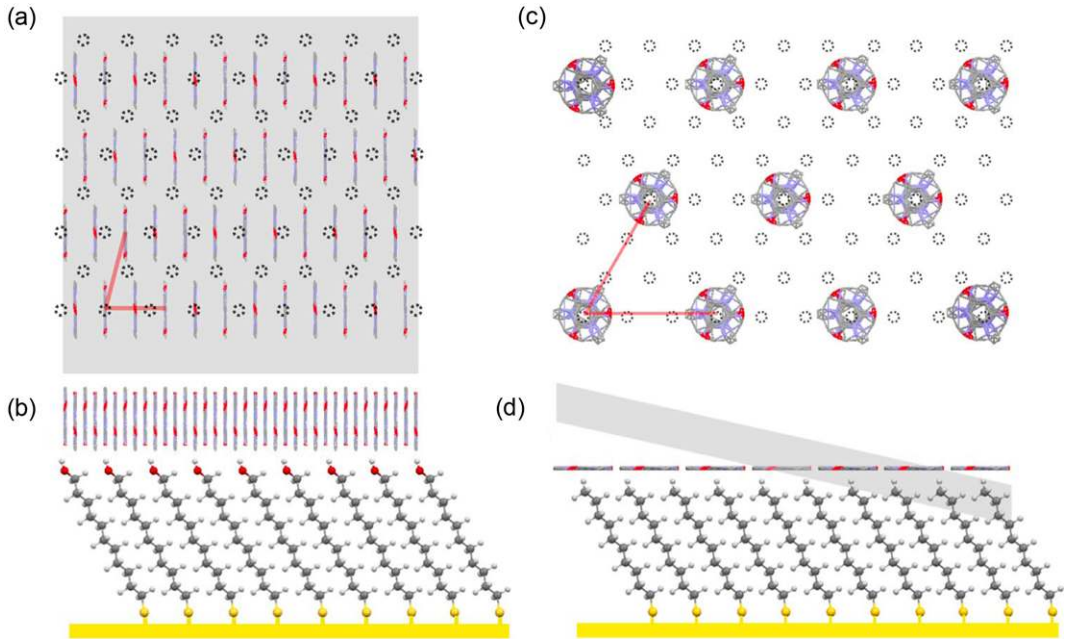

Fig. 5. Schematic representations of the nucleating molecular layers of caffeine on SAM-OH, (a) top view and (b) side view, and on SAM-CH_3, (c) top view and (d) side view. The (2 –1 0) plane parallel to the SAM-OH surface was shown in (a), and the (1 0 –2) plane angled to the SAM-CH_3 surface was shown in (d). In (a) and (c), the dotted circle represents the terminal hydrogen of SAMs, and two red lines connect the equivalent caffeine molecules in the molecular layers.

phology of three selective theobromine crystals. The truncated pyramidal crystals surrounded by two equivalent {0 2 1} and two other equivalent {−1 2 0} side faces with a {−2 0 2} top face are consistent with the strong intensity of the (−2 0 2) X-ray diffraction as well as the morphological observation.

To understand the nucleation phenomena on SAMs, observed for caffeine and theobromine, probable molecular interactions between the end groups of SAMs and crystallizing molecules were explored. The SAMs in the present study are known to form $(\sqrt{3}\times\sqrt{3})R29^{\circ}$ structures with a twist angle ca. 55° and a tilt angle ca. 29°, which orients the terminal hydrogens in such a way as to participate in the interfacial interactions with the nucleating molecules of caffeine and theobromine [28-30]. Caffeine and theobromine are tri- and di-methylated xanthines; caffeine has an additional methyl group on one of Ns in the six-membered ring, where theobromine has only hydrogen (Fig. 4(a)). Since the caffeine molecule does not have a strong donor of hydrogen bonding, its packing in its own crystal, relying on π-stacking, possesses severe disorder. In particular, the α polymorph, observed in this study on SAMs, contains a massive whole-molecule disorder (Fig. 4(b)). [26] In contrast, theobromine molecules experience extensive hydrogen bonding among them to generate two-dimensional hydrogen-bonded layers (Fig. 4(c)), which are in turn held by weaker intermolecular interactions [25]. Especially, N-H···O=C hydrogen bonds within the two-dimensional networks contribute to form stable dimer structures.

Based on the SEM and XRD observations, more reliable interactions appear to exist for caffeine with SAM-OH (and SAM-COOH) and for theobromine with SAM-CH_3. The difference in the reliable interfacial interaction seems to arise from the structural dissimilarities in caffeine and theobromine mentioned previously. The specific origin of this difference becomes obvious when the possible inter-

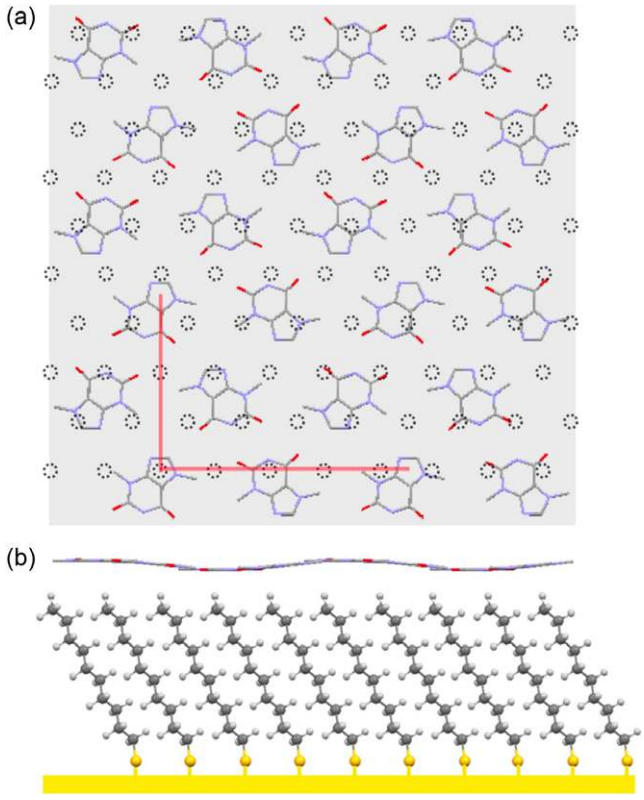

Fig. 6. Schematic representation of the nucleating molecular layer of theobromine on SAM-CH_3: (a) top view and (b) side view. The (–2 0 2) plane parallel to the SAM-CH_3 surface was shown in (a). The dotted circle represents the terminal hydrogen of SAM-CH_3, and two red lines connect the equivalent theobromine molecules in the molecular layer.

action sites of caffeine and theobromine, such as O=C and π (imidazole), are examined in terms of orientation favorable to interact with the terminal hydrogens of SAMs (Note that the SAMs were prepared via absolute ethanol solutions, and caffeine or theobromine was sublimated onto the SAMs to prevent complicated intermolecular interaction scenarios, such as solvent participation and ionization.).

Caffeine interacts with SAM-OH and SAM-COOH via OH···O=C hydrogen bonding. Figs. 5(a) (top view) and 5(b) (side view) show one of the probable interactions between SAM-OH and caffeine. The molecular plane of caffeine is shown perpendicular to the (2 −1 0) plane (gray square in Fig. 5(a)), which is consistent with the strong (2 −1 0) X-ray diffraction peak and the microscopically observed needle orientation. No apparent epitaxy can be found in Fig. 5(a), where dotted circles represent the terminal hydrogens of SAM-OH, and two red lines connect the equivalent caffeine molecules in the molecular layer displayed. Also, in the representation of Fig. 5(b), the OH···O=C interaction does not have linear geometry that would require the molecular layer to tilt away from the SAM-OH surface (for clarity only the front row SAM-OH molecules are shown in Fig. 5(b)). Bringing the molecular layer parallel to the SAM-OH surface by sacrificing the linearity of hydrogen bonding would ensure multiple OH···O=C interactions to maximize the interfacial interactions. The cooperative behavior of the caffeine molecular layer may originate from the fact that the caffeine molecules are π-stacked within the layer parallel to the *c* direction. SAM-COOH would have similar interactions with a slightly different tilt angle of the terminal hydrogen of the SAM molecules.

In contrast, caffeine interacts with SAM-CH_3 via CH···π as well as CH···O=C interactions. Figs. 5(c) (top view) and 5(d) (side view) show the probable CH···π interactions between SAM-CH_3 and caffeine. While the disorder in caffeine crystals makes it difficult to pinpoint the position of the π-conjugated imidazole ring, the hexagonally packed caffeine molecules have a structure close to the coincidence epitaxy to the underlying SAM-CH_3. The terminal hydrogen and the caffeine molecular plane are slightly angled, not orthogonal, to make the epitaxy relationship possible. This configuration explains the microscopically observed caffeine needles standing on the nucleating SAM-CH_3 surfaces. Also, the slightly angled (1 0 −2) plane (grey plane in Fig. 5(d)) is consistent with the weak (1 0 −2) diffraction peak. The microscopic observation of the tilt angle variation of the caffeine needles may arise from the combination of the weak intermolecular interactions within the caffeine molecular layer and the weak CH···π interfacial interactions (Note that the CH···π interaction is known to have a shallow energy minimum to easily accommodate some geometrical variation [21]. Also, :N of the imidazole ring may form a part of the combined hydrogen-bonding acceptor [31].). We also note that the SAM-CH_3 is capable of interacting with caffeine molecules through CH···O=C interactions in a similar fashion to the SAM-OH case, which is consistent with the mixed crystal orientation observed for this substrate. Although the individual interaction is probably stronger for CH···O=C than for CH···π, the possible coincidence epitaxy for the case of CH···π, combined with :N- contribution, appears to slightly favor the latter interaction overall to form more than half of the crystal needles on SAM-CH_3 in the standing orientation. Similar phenomenon of mixed orientation was not observed for SAM-OH and SAM-COOH, probably because the OH···O=C interactions with the well π-stacked caffeine molecules were too much stronger to allow OH···π interactions to persist during crystal nucleation.

Theobromine interacts with SAM-CH_3 predominantly via CH···π interaction. A probable interaction model is shown in Figs. 6(a) (top view) and 6(b) (side view) that is consistent to the strong (−2 0 2) X-ray diffraction and the truncated pyramidal morphology observation. The theobromine molecules nearly parallel to the (−2 0 2) plane (gray square in Fig. 6(a)) form the two-dimensional hydrogen-bonded layer as described previously, which induces the molecular network to behave cooperatively to maximize the the CH···π interactions, maintaining the strong intra-layer hydrogen bonds but altering the orthogonal geometry of weak CH···π interactions. Note that no apparent epitaxy relationship can be found between SAM-CH_3 and theobromine. In contrast to the case of caffeine on SAM-CH_3, other crystal orientation due to the possibly competing CH···O=C interaction was not observed experimentally. This critical difference appears to arise from the structural coherence of the interacting molecular layer, which strongly exists for the extensively hydrogen-bonded theobromine molecules, but not for the caffeine molecules held by weaker interactions (Figs. 6(a) and 5(c)).

Theobromine interactions with SAM-OH and SAM-COOH are hard to analyze because of the lack of the distinctive diffraction patterns as well as the seemingly diverse crystal orientation (Figs. 1(e) and 1(f)). At least two different orientations of specific interactions are possible, one being via OH···π interaction similarly observed with SAM-CH_3 and the other through OH···O=C interactions. The former geometry has the (−2 0 2) plane in an X-ray diffracting position in the θ-2θ mode, but the latter configuration effectively reduces the (−2 0 2) diffraction, which is consistent with the experimental observations. Also, these interfacial interactions appear to compete comparably to nucleate theobromine crystals, which explains the modest batch-to-batch variation in these heterogeneous nucleations while a significant reduction in the (−2 0 2) diffraction peak was consistently observed. This behavior of theobromine on SAM-OH or SAM-COOH is quite different from the stable caffeine orientation control on the same substrates. The contrast between theobromine and caffeine may originate from the interplay between the interfacial interactions and the in-plane coherence of the nuclei. The OH···O=C interfacial interaction allows caffeine molecules to assemble with stronger intra-layer interactions than the interlayer interactions, as explained previously (Fig. 5). However, the same interfacial interaction requires theobromine molecules to experience weaker intra-layer interactions (long non-conventional H-bonds) than their interlayer interactions (extensive networks of short conventional H-bonds and intermediate non-conventional H-bonds) [25].

CONCLUSIONS

We have successfully utilized SAMs of different functional groups to control the orientation of caffeine and theobromine crystals. The orientation-regulated crystal nucleation mainly depended on stereochemistry via specific interactions between the SAM functional groups and the crystallizing molecules. The specific interfacial interactions were diversely found as strong hydrogen bonding, non-conventional hydrogen bonding with π acceptors, and CH/π interactions. Surprisingly, well-oriented crystals were obtained with the weak CH/π interactions for theobromine, which did not have appar-

ent epitaxy with the SAM substrate. We believe this phenomenon is closely related to the cohesiveness of the theobromine molecular layers parallel to the substrate that would initially form as a part of crystal nuclei. The strongly cohesive layer would require its multiple interfacial interactions to behave cooperatively, which in turn ensures reliable formation of oriented nuclei. Without similar cohesiveness, the same CH/π interactions did not generate stable orientation control with caffeine molecules even with the coincidence-type epitaxy with the SAM substrate. Mixed orientations were found in this case. Conversely, strong hydrogen bonding between caffeine and SAM-OH or SAM-COOH, combined with the cooperatively interacting molecular layer, ensured the undivided orientation control, whereas the same strong hydrogen bonding with theobromine, without strongly cohesive molecular structure parallel to the substrate, did not induce uniformly oriented crystals. Our conclusion indicates that, at least for the systems in the present study, the nuclei or precursors of crystallization require cohesive structures parallel to the nucleating substrates to utilize specific interfacial interactions to control the crystal orientation in a concerted manner. We believe this consideration is especially important for the oriented crystallization of organic molecules, where diverse weak interactions exist in their crystal structures.

ACKNOWLEDGEMENT

This research was supported by Basic Science Research Program through the National Research Foundation of Korea (NRF) funded by the Ministry of Education, Science and Technology (2009-0075243).

REFERENCES

1. H. A. Lowenstam and S. Weiner, *On Biomineralization*, Oxford University Press, New York (1989).
2. S. Weiner and L. Addadi, *J. Mater. Chem.*, **7**, 689 (1997).
3. M. Sarikaya, C. Tamerler, A. K. Y. Jen, K. Schulten and F. Baneyx, *Nat. Mater.*, **2**, 577 (2003).
4. X. Li, W.-C. Chang, Y. J. Chao, R. Wang and M. Chang, *Nano Lett.*, **4**, 613 (2004).
5. J. Aizenberg, A. Tkachenko, S. Weiner, L. Addadi and G. Hendler, *Nature*, **412**, 819 (2001).
6. S. Mann, *Biomineralization: Principles and concepts in bioinorganic materials chemistry*, Oxford University Press, New York (2001).
7. G. S. Fu, R. Qiu, C. A. Orme, D. E. Morse and J. J. De Yoreo, *Adv. Mater.*, **17**, 2578 (2005).
8. I. W. Kim, M. R. Darragh, C. Orme and J. S. Evans, *Cryst. Growth Des.*, **6**, 5 (2006).
9. I. W. Kim, J. L. Giocondi, C. Orme, S. Collino and J. S. Evans, *Cryst. Growth Des.*, **4**, 1154 (2008).
10. A. M. Belcher, X. H. Wu, R. J. Christensen, P. K. Hansma, G. D. Stucky and D. E. Morse, *Nature*, **381**, 56 (1996).
11. F. F. Amos and J. S. Evans, *Biochemistry*, **48**, 1331 (2009).
12. S. Weiner and W. Traub, *FEBS Lett.*, **111**, 301 (1980).
13. L. Addadi and S. Weiner, *Proc. Natl. Acad. Sci. USA*, **82**, 4110 (1985).
14. C. A. Orme, A. Noy, A. Wierzbicki, M. T. McBride, M. Grantham, H. H. Teng, P. M. Dove and J. J. DeYoreo, *Nature*, **411**, 775 (2001).
15. J. Aizenberg, A. J. Black and G. M. Whitesides, *J. Am. Chem. Soc.*, **121**, 4500 (1999).
16. Y.-J. Han, L. M. Wysocki, M. S. Thanawala, T. Siegrist and J. Aizenberg, *Angew. Chem. Int. Ed.*, **44**, 2386 (2005).
17. P. W. Carter and M. D. Ward, *J. Am. Chem. Soc.*, **115**, 11521 (1993).
18. E. I. Givargizov, M. O. Kliya, V. R. Melik-Adamyan, A. I. Grebenko, R. C. DeMattei and R. S. Feigelson, *J. Cryst. Growth*, **12**, 758 (1991).
19. B. Pokroy, V. F. Chernow and J. Aizenberg, *Langmuir*, **25**, 14002 (2009).
20. J. F. Kang, J. Zaccaro, A. Ulman and A. Myerson, *Langmuir*, **16**, 3791 (2000).
21. G. R. Desiraju and T. Steiner, *The weak hydrogen bond in structural chemistry and biology*, Oxford University Press, New York (1999).
22. T. Steiner and G. Koellner, *J. Mol. Biol.*, **295**, 535 (2001).
23. K. F. Bowes, I. P. Clark, J. M. Cole, M. Gourlay, A. M. E. Grifn, M. F. Mahon, L. Ooi, A. W. Parker, P. R. Raithby, H. A. Sparkes and M. Towrieb, *Cryst. Eng. Commun.*, **7**, 259 (2005).
24. C. A. Bessel, R. F. See, D. L. Jameson, M. R. Churchill and K. J. Takeuchi, *J. Chem. Soc., Dalton Trans.*, 3123 (1992).
25. K. A. Ford, Y. Ebisuzaki and P. D. Boyle, *Acta Cryst.*, **C54**, 1980 (1998).
26. G. D. Enright, V. V. Terskikh, D. H. Brouwer and J. A. Ripmeester, *Cryst. Growth Des.*, **7**, 1406 (2007).
27. I. W. Kim, R. E. Robertson and R. Zand, *Adv. Mater.*, **15**, 709 (2003).
28. Y. Qian, G. Yang, J. Yu, T. A. Jung and G.-Y. Liu, *Langmuir*, **19**, 6056 (2003).
29. Y.-C. Yang, T.-Y. Chang and Y.-L. Lee, *J. Phys. Chem. C*, **111**, 4014 (2007).
30. S. M. Mendoza, I. Arfaoui, S. Zanarini, F. Paolucci and P. Rudolf, *Langmuir*, **23**, 582 (2007).
31. S. Kumar, K. Subramanian, R. Srinivasan, K. Rajagopalan and T. Steiner, *J. Mol. Struct.*, **471**, 251 (1998).